The Journal of Immunology

Irf4 Expression in Thymic Epithelium Is Critical for Thymic Regulatory T Cell Homeostasis

Uku Haljasorg, James Dooley, Martti Laan, Kai Kisand, Rudolf Bichele, Adrian Liston and Pärt Peterson

J Immunol 2017; 198:1952-1960; Prepublished online 20 January 2017;
doi: 10.4049/jimmunol.1601698
http://www.jimmunol.org/content/198/5/1952

The Journal of Immunology is published twice each month by
The American Association of Immunologists, Inc.,
1451 Rockville Pike, Suite 650, Rockville, MD 20852

Print ISSN: 0022-1767 Online ISSN: 1550-6606.

Irf4 Expression in Thymic Epithelium Is Critical for Thymic Regulatory T Cell Homeostasis

Uku Haljasorg,* James Dooley,† Martti Laan,* Kai Kisand,* Rudolf Bichele,* Adrian Liston,† and Pärt Peterson*

The thymus is a primary lymphoid organ required for the induction and maintenance of central tolerance. The main function of the thymus is to generate an immunocompetent set of T cells not reactive to self. During negative selection in the thymus, thymocytes with autoreactive potential are either deleted or differentiated into regulatory T cells (Tregs). The molecular basis by which the thymus allows high-efficiency Treg induction remains largely unknown. In this study, we report that IFN regulatory factor 4 (Irf4) is highly expressed in murine thymic epithelium and is required to prime thymic epithelial cells (TEC) for effective Treg induction. TEC-specific Irf4 deficiency resulted in a significantly reduced thymic Treg compartment and increased susceptibility to mononuclear infiltrations in the salivary gland. We propose that Irf4 is imperative for thymic Treg homeostasis because it regulates TEC-specific expression of several chemokines and costimulatory molecules indicated in thymocyte development and Treg induction.
***The Journal of Immunology*, 2017, 198: 1952–1960.**

Thymic stroma provides a unique microenvironment for the stepwise maturation of thymocytes that give rise to peripheral T cell populations. Following the positive selection of $CD4^+CD8^+$ double-positive thymocytes by cortical thymic epithelial cells (cTEC), the migration of positively selected thymocytes to the thymic medulla is dependent on chemokines that act as ligands for CCR4 and CCR7 (1, 2). Medullary TEC (mTEC), which comprise $CD80^{lo}$MHC class II (MHC-II)^{lo} ($mTEC^{lo}$) and $CD80^{hi}$ MHC-II^{hi} ($mTEC^{hi}$) populations, are, along with thymic dendritic cells (DC), responsible for negative selection of autoreactive $CD4^+$ $CD8^-$ single-positive (SP; CD4 SP) and $CD4^-CD8^+$ (CD8 SP) thymocytes. Negative selection driven by mTEC is largely dependent on autoimmune regulator (Aire) expressed in $mTEC^{hi}$, which induces the expression of thousands of tissue-specific Ags (TSA) that are presented in complex with MHC on $mTEC^{hi}$ cells to the maturing thymocytes (3–6). The maturation program and specific gene expression patterns of TEC that are needed to facilitate T cell selection have been shown to be dependent on several TNF superfamily (TNFSF) members, produced by maturing thymocytes as demonstrated by studies in mice lacking receptor activator of NF-κB (RANK), RANK ligand (RANKL), CD40, lymphotoxin β (LTb), as well as RANKL in combination with CD40 or LTbR (7–9).

Thymocytes undergoing negative selection require costimulation from several molecules expressed on mTEC such as CD40, CD80, and CD86, which provide additional signaling to the maturing conventional T cells and regulatory T cells (Tregs) (10). As a result of negative selection, thymocytes recognizing self-peptides as foreign are either deleted or differentiated into Tregs (11, 12). Aire deficiency as well as alterations in the expression pattern of mTEC chemokines and costimulatory molecules result in anomalous thymic Treg profiles (13–16). In addition to Tregs generated in the thymus (tTregs) CD4 SP $Foxp3^-$ cells encountering a self-antigen or a tolerizing foreign Ag outside the thymus can differentiate into peripherally induced Tregs (pTregs) that lack Helios and Neuropilin 1 (Nrp1) expression in steady-state (17–20).

IFN regulatory factor 4 (Irf4) is a member of a family of transcription factors consisting of nine members with distinct functions in both innate and adaptive immunity (21). Unlike several other members of the family, *Irf4* is not induced by IFN signaling; rather, its expression is activated by extracellular stimuli leading to NF-κB activation. In thymocytes (22) and peripheral T cells, *Irf4* expression is upregulated following TCR signaling, and most effector T cell populations, including Tregs, are dependent on Irf4 expression (reviewed in Ref. 23).

Irf4 has multiple roles in the differentiation and function of professional APC from lymphoid and myeloid lineages. In B cells, *Irf4* expression can be induced by IL-4 and CD40 costimulation and Ag binding (24–26). Although not impaired in Ag uptake, Irf4-deficient murine B cells fail to upregulate *Aicda* expression, and subsequently Irf4-deficient mice lack germinal centers and plasma cells (27, 28). Among APC from the myeloid lineage, Irf4 has been shown to be critical for the development of the $CD4^+$ $CD11b^{hi}$ DC population and M2 macrophage differentiation (29, 30). In human monocytes differentiating into DC, *Irf4* expression is dependent on NF-κB signaling following GM-CSF and IL-4 stimulation and is upregulated upon encountering foreign Ag (31). Irf4 deficiency in $CD11b^{hi}$ DC results in failed upregulation of MHC-II expression and abolishment of their function as APC (29) and Th17 polarizing capacity (32). Furthermore, Irf4 controls

*Institute of Biomedicine and Translational Medicine, University of Tartu, 50411 Tartu, Estonia; and †Department of Microbiology and Immunology, KU Leuven, Leuven 3000, Belgium

ORCIDs: 0000-0002-1541-6020 (U.H.); 0000-0003-3154-4708 (J.D.).

Received for publication October 3, 2016. Accepted for publication December 26, 2016.

This research was supported by the European Union through the European Regional Development Fund (Project 2014-2020.4.01.15-0012) and by Estonian Research Council Grant IUT2-2.

Address correspondence and reprint requests to Uku Haljasorg, University of Tartu, Ravila 19, 50411 Tartu, Estonia. E-mail address: uku.haljasorg@ut.ee

The online version of this article contains supplemental material.

Abbreviations used in this article: Aire, autoimmune regulator; cKO, conditional knockout; cTEC, cortical thymic epithelial cell; DC, dendritic cell; FTOC, fetal thymic organ culture; Irf4, IFN regulatory factor 4; Ivl, Involucrin; Krt14, keratin 14; LTb, lymphotoxin β; MHC-II, MHC class II; mTEC, medullary TEC; $mTEC^{hi}$, $CD80^{hi}$MHC-II^{hi}; $mTEC^{lo}$, $CD80^{lo}$MHC class II^{lo}; Nrp1, Neuropilin 1; pTreg, peripherally induced Treg; qPCR, quantitative PCR; RANK, receptor activator for NF-κB; RANKL, RANK ligand; SP, single-positive; TEC, thymic epithelial cell; TNFSF, TNF superfamily; Treg, regulatory T cell; TSA, tissue-specific Ag; tTreg, Tregs generated in the thymus; WT, wild-type.

the expression of several marker genes required for the antihelminthic function of M2 macrophages (30).

Although Irf4 plays a critical role in the development and/or function of both lymphoid and myeloid APC, its potential functional role in stromal APC such as mTEC remains elusive. In this study, we report high expression of Irf4 in TEC that have a central role in self-antigen presentation. To study Irf4 function in TEC, we generated conditional knockout (cKO) mice lacking functional Irf4 specifically in the thymic epithelium (named Irf4-cKO here). We found that *Irf4* expression in the thymic epithelium was specifically controlled by RANK signaling, and the mTEC compartment in Irf4-cKO mice was skewed toward the mTEC^{hi} population. Irf4-deficient mTEC^{hi} were impaired in their ability to generate Tregs, as the percentage of thymic Tregs in Irf4-cKO mice was significantly decreased. This change was accompanied by an imbalance in the expression of several chemokines and costimulatory molecules in mTEC^{hi} required for Treg development. Furthermore, although the decrease in Tregs was homeostatically compensated in the periphery, aged Irf4-cKO mice were susceptible to mononuclear infiltrations in their salivary glands, insinuating a functional restriction in the peripheral compensated Treg pool.

Materials and Methods

Mice

All mice were maintained and animal experiments performed at the Vivarium of the Institute of Biomedicine and Translational Medicine, University of Tartu. A TEC-specific conditional Irf4-deficient mouse strain was generated by crossing B6.129S1-*Irf4*^{tm1Rdf}/J (Irf4$^{fl/fl}$) (named wild-type [WT] here) (The Jackson Laboratory) and FoxN1:Cre mice (a gift from Thomas Boehm). F_1 mice heterozygous for FoxN1:Cre and Irf4^{fl} were crossed with B6.129S1-*Irf4*^{tm1Rdf}/J mice. Mice from F_2 progeny lacking the first two exons of Irf4 and expressing GFP in FoxN1:Cre-expressing tissues were used in experiments. Genotypes were determined by PCR using primers specific for the second exon of Irf4 (sequences are available on The Jackson Laboratory Web site). FoxN1 and Irf4 are indicated in dermal cells (33, 34). No visual phenotype was observed even in aged F_2 mice (52 wk old). C57BL/6 mice deficient for the *Aire* gene were generated as previously described at the Walter and Eliza Hall Institute for Medical Research by a targeted disruption of the Aire gene in exon 8. The mice were maintained and crossed as Aire$^{+/-}$ mice. In all experiments, male and female mice were used in equal proportions. All animal experiments were approved by the Ethical Committee on Animal Experiments at the Ministry of Agriculture, Estonia.

Flow cytometric and FACS analysis

For purification, thymi from 8- to 10-wk-old Irf4-cKO and WT or 4- to 6-wk-old Aire-KO mice and their littermate Aire-WT controls were minced and gravity sedimented several times in RPMI 1640 media containing 2% FBS and 20 mM HEPES. The enriched stromal compartment from each genotype was pooled and enzymatically digested in RPMI 1640 media containing collagenase 2 (125 U/ml; Life Technologies) and DNase 1 (15 U/ml; AppliChem) for 20 min at room temperature followed by two 20-min digestions with collagenase 2, DNase 1, and Dispase (0.75 U/ml; Life Technologies). Following FcR blocking with 2.4G2 hybridoma medium, thymocytes were stained for FACS sorting or flow cytometric analysis. The enriched stromal compartment was sorted into TRIzol LS reagent (Life Technologies) with FACSAria (BD Biosciences). TEC subpopulations were determined as follows: mTEC^{lo}, CD45$^-$EpCam$^+$Ly51$^-$MHC^{lo}; mTEC^{hi}, CD45$^-$EpCam$^+$Ly51$^-$MHC^{lo}; cTEC, CD45$^-$EpCam$^+$Ly51$^+$. For thymocyte and lymphocyte analysis, thymi and spleens were homogenized using glass slides, and erythrocytes in the spleens were lysed using osmotic shock: cells were resuspended in 900 μl of deionized water, and 100 μl of 10× PBS was added after 10 s. Cells were strained, counted, incubated in 2.4G2 FcR-blocking medium, stained, and cells for all experiments were analyzed using LSRFortessa flow cytometer with FACSDiva software (BD Biosciences) or FCS Express 5 Flow (De Novo Software). A list of Abs used in the study is available on request.

Fetal thymic organ culture

Fetal thymic organ cultures (FTOCs) were established from embryonic day 16.5 mouse embryos and performed as described earlier (9). Following thymocyte depletion with 2′-deoxyguanosine treatment for 6 d, one lobe from each thymus was cultured for 24 h on DMEM alone, the other on DMEM with 500 ng/ml RANKL (eBioscience). To test the effect of NF-κB inhibitors on Irf4 expression, FTOCs were prepared using the aforementioned method from C57BL/6 mice. After 6 d, thymocyte-depleted FTOCs were treated with inhibitors for IKK-β (TPCA-1; Tocris Bioscience) or NIK [isoquinoline-1,3(2H,4H)-dione; Santa Cruz Biotechnology] at indicated concentrations with or without 500 ng/ml RANKL.

RNA purification and quantitative PCR

RNA purification was carried out using RNeasy micro kits (Qiagen) according to the manufacturer's protocols, followed by reverse transcription using SuperScript III reverse transcriptase (Life Technologies). All quantitative PCRs (qPCRs) were carried out on a ViiA 7 real-time PCR system. Every sample was run in three parallel reactions. Relative gene expression levels were calculated using the comparative Ct (ΔΔCt) method (according to Applied Biosystems), where the relative expression is calculated as $2^{-\Delta\Delta Ct}$, and where Ct represents the threshold cycle. β_2-Microglobulin and cytokeratin 8 were used as housekeeping genes for normalization. A list of primers used in this study is available upon request.

Immunofluorescence

Immunofluorescence was performed on frozen sections fixed with acetone or 4% formaldehyde. Formaldehyde-fixed tissues were permeabilized with 0.1% Triton X-100 in PBS. A 30-min blocking step at room temperature with 1% normal goat serum was used. Sections were incubated overnight with indicated primary Ab at 4°C, washed in PBS, and incubated with a respective secondary Ab (1:1000) for 60 min at room temperature. Slides were washed four times with PBS, stained with DAPI (1 μg/ml) where indicated for 10 min, washed once more in PBS, and covered with fluorescent mounting medium (Dako) and coverslips. Images were obtained with an LSM 710 microscope (Zeiss).

Mononuclear infiltrations

Livers, pancreases, and salivary glands from aged mice (8–10 mo) were isolated, fixed in 4% paraformaldehyde in PBS, embedded in paraffin, cut into 5-μm sections, and stained with H&E. Images were obtained with an Eclipse Ci microscope (Nikon).

Statistical analysis

Statistical significance for flow cytometry and qPCR analysis was determined by a two-tailed unpaired *t* test and for infiltrates by a two-tailed Mann–Whitney *U* test using Prism from GraphPad Software (La Jolla, CA).

Results

RANK signaling during development induces Irf4 in the thymic epithelium

DC and B cells, representing professional APC, display impaired differentiation and Ag presentation under Irf4-deficient conditions (24, 27, 28). Owing to their APC-like properties and pivotal role in central tolerance induction, we sought to characterize the role of Irf4 in TEC. From sorted WT TEC (see sorting strategy in Supplemental Fig. 1A), we found the expression of *Irf4* mRNA in all three major TEC populations, with highest levels in mTEC^{hi} (Fig. 1A). At the protein level, the highest expression of Irf4 was also detected in mTEC^{hi} (Fig. 1B, see gating in Supplemental Fig. 1B), with close to two-thirds of the cells being positive for Irf4. Roughly a third of both mTEC^{lo} and cTEC were positive for Irf4, in agreement with the lower level of *Irf4* mRNA expression in these cells.

The maturation and gene expression profile of the thymic epithelial compartment has been shown to depend on signals received from developing thymocytes (35). To identify the specific ligands for TNFSF receptors that drive *Irf4* expression in the thymic epithelium we used FTOCs, which we stimulated with several ligands known to have a functional role in TEC maturation. The results from 2′-deoxyguanosine–treated FTOCs showed strong induction of *Irf4* expression in TEC after RANKL stimulation (Fig. 1C). Among the other TNFSF members analyzed (CD40L, Light, TNF-α, LTbR agonist), CD40 has been shown to induce

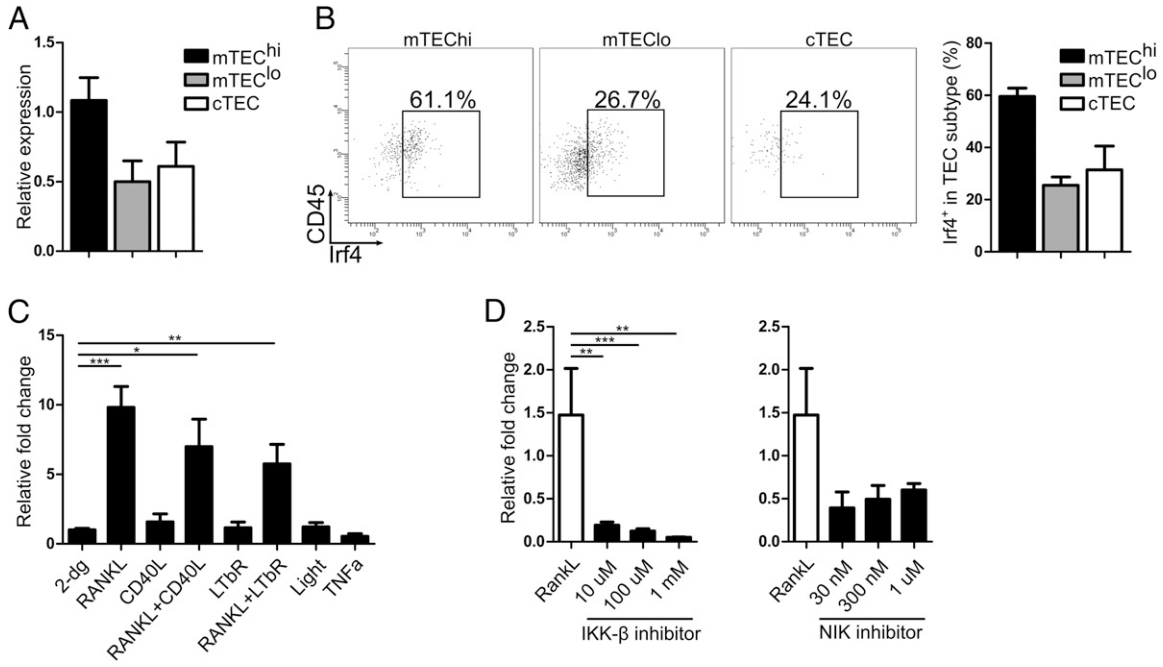

FIGURE 1. Thymic epithelium constitutively expresses Irf4. (**A**) Relative *Irf4* mRNA expression level in WT TEC subsets. (**B**) Irf4 protein expression in WT TEC subsets. Data are representative of two experiments from pooled WT thymi from four mice and are shown as means + SEM. (**C**) Relative *Irf4* mRNA expression in 2′-deoxyguanosine (2-dg)–treated WT FTOC thymi following stimulation with the indicated TNFSF member for 24 h. For each embryo, the expression of *Irf4* was compared between the untreated and treated lobe of the same thymus. (**D**) Relative *Irf4* mRNA expression in WT FTOC stimulated for 24 h with RANKL or a combination of RANKL and inhibitors with high specificity for IKK-β (left) or NIK (right) at indicated concentrations. Data are shown as the means + SEM of three to five replicates with material from two pooled thymic lobes making up one sample. $*p \leq 0.05$, $**p \leq 0.01$, $***p \leq 0.001$, unpaired *t* test, two-tailed.

Irf4 expression in both germinal center B cells and DC (24, 36). However, CD40 had a negligible effect on TEC-specific upregulation of *Irf4* expression. We also studied RANKL costimulation with CD40 or LTbR, as we have previously observed a synergistic effect on the expression of *Aire* and *Fezf2* genes in TEC (37); however, the costimulation had no additive effect on *Irf4* expression in FTOCs.

To determine which NF-κB pathway is induced downstream of RANK signaling and activates *Irf4* expression in TEC, we treated RANK-induced FTOCs either with TPCA-1, a classical NF-κB pathway inhibitor with high selectivity for IKK-β over IKK-α, or a selective NIK inhibitor [isoquinoline-1,3(2H,4H)-dione], which blocks the alternative NF-κB pathway. Inhibiting the classical pathway resulted in a substantial downregulation even at low concentrations of the IKK-β inhibitor (Fig. 1D), whereas using the NIK inhibitor resulted in a nonsignificant but strongly trending decrease in *Irf4* expression. Based on these results, we concluded that the thus far undescribed *Irf4* expression in TEC is constitutive and that components from the classical NF-κB pathway are critical for the activation of Irf4 downstream of RANK–RANKL binding.

Irf4 induction restrains the differentiation of thymic epithelium

We next generated TEC-specific Irf4-deficient mice by crossing $Irf4^{fl/fl}$ mice (28) (referred to here as WT) with FoxN1:Cre mice. A proportion of the F_2 progeny of these mice are deficient in *Irf4* expression and express *GFP* in tissues coexpressing *FoxN1:Cre* and *Irf4* (referred to here as Irf4-cKO). The effectiveness of excision of the first two exons of Irf4 was demonstrated by comparable levels of TEC subtypes in Irf4-cKO–expressing GFP (Fig. 2A) and Irf4-expressing TEC in the WT mice (Fig. 1A). We verified Irf4 protein expression by immunofluorescence analysis, which shows Irf4 in the medulla of WT mice to locate mainly in keratin 14 $(Krt14)^+$ cells (Supplemental Fig. 1C), whereas in Irf4-cKO mice cells coexpressing Krt14 and Irf4 are virtually absent. Scarce $Krt14^-$ cells expressing Irf4 in Irf4-cKO could either be CD4 SP cells or DC (22, 38). No differences were found in the general cellularity of the thymi of WT and Irf4-cKO mice, and our flow cytometry analysis from these mice revealed the only differences in the stromal compartment to be the significantly decreased $mTEC^{lo}/mTEC^{hi}$ ratio in the Irf4-cKO mice (Fig. 2B, Supplemental Fig. 1D). To determine whether this increase in the $mTEC^{hi}$ population translated into major changes in the maturation of mTEC or aberrant thymic architecture, we analyzed thymic sections from WT and Irf4-cKO mice by immunofluorescence. Stainings for mTEC marker Krt14, mature mTEC marker UEA-1, or terminally differentiated TEC positive for Involucrin (Ivl) revealed no robust differences between the genotypes (Fig. 2C, Supplemental Fig. 1E). Taken together, these results suggest that Irf4 regulates the $mTEC^{lo}$ to $mTEC^{hi}$ transition.

Irf4 expression by thymic epithelium is essential for priming thymic epithelium into efficient Treg inducers

To determine whether the altered medullary phenotype combined with Irf4 deficiency influences the maturation of thymocytes, we studied the distribution of thymocyte and peripheral T cell subpopulations by flow cytometry. The distribution of CD4 SP and CD8 SP populations as well as double positive and double negative (Fig. 3A) and double negative thymocyte subtypes (data not shown) were comparable in the thymi of 8- to 10-wk-old WT and Irf4-cKO mice. Analysis of the spleens (Fig. 3A) and lymph nodes (data not shown) of Irf4-cKO mice showed the distribution of SP T cells to be similar to the WT. However, analysis of the thymic $Foxp3^+$ population revealed a 50% decrease in the Treg population within CD4 SP cells (Fig. 3B). No differences were found in splenic $Foxp3^+$ Treg percentages (Fig. 3C) or Foxp3 expression

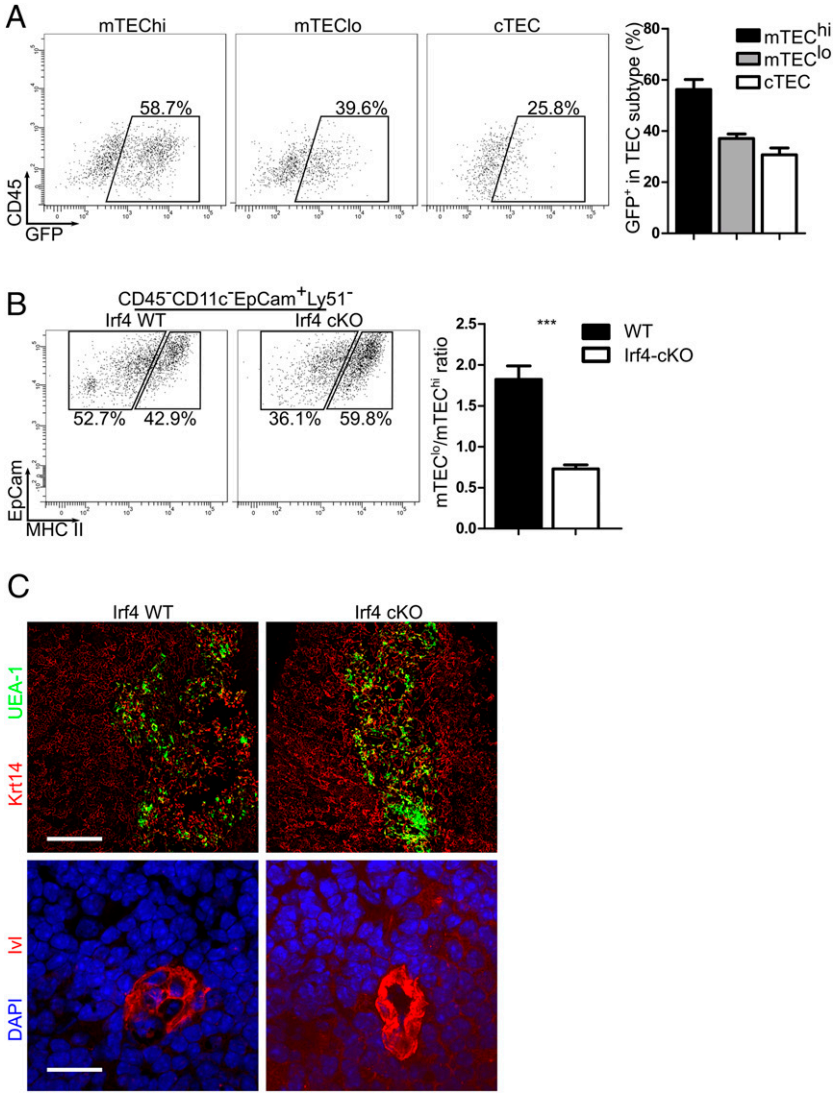

FIGURE 2. Irf4 regulates mTEC maturation. (**A**) GFP-protein expression in Irf4-cKO TEC subsets occurring after the excision of the first two exons of Irf4. (**B**) The percentages of mTEC subpopulations in WT and Irf4-cKO mice were evaluated by flow cytometry. Plots shown for (A) and (B) are representative of four independent experiments. Data from (A) and (B) are shown as the means + SEM from four independent experiments with pooled thymi ($n = 3–6$). ***$p \leq 0.001$, unpaired t test, two-tailed. (**C**) Thymic sections from WT and Irf4-cKO mice were stained for Krt14 (mTEC), UEA-1 (mature mTEC) (scale bar, 200 μm), and Inl (terminally differentiated TEC) (scale bar, 20 μm). Images shown are representative of three mice per genotype from two independent experiments.

levels in the thymi or spleens (Supplemental Fig. 1F). The peripheral compensation of Tregs in Irf4-cKO is likely homeostatic, as Treg numbers that were decreased in the thymi of Irf4-cKO were also restored to WT levels in the spleen (Fig. 3D). To determine whether the decrease in Tregs observed in the thymus could be the result of decreased proliferation, we analyzed Ki-67 expression in Tregs. In fact, a larger proportion of both thymic and splenic Tregs in Irf4-cKO expressed the proliferation marker Ki-67 (Fig. 3E). Analysis of CD44 and CD62L expression on splenic Tregs (Fig. 3F) revealed that the size of the activated Treg population ($CD44^+CD62L^-$) was comparable in WT and Irf4-cKO mice, but in Irf4-cKO mice we saw a slight but significant decrease in resting ($CD44^-CD62L^+$) Tregs. Overall, these data identify Irf4 in mTEC as a critical factor required for sustained thymic Treg production.

Blockade of the RANKL–Irf4 pathway in thymic epithelium forces reliance on pTregs and enhanced susceptibility to mononuclear infiltrations

tTregs, but not pTregs, express Helios and Nrp1 in steady-state (19). We defined tTregs as cells coexpressing Nrp1 and Helios, as suggested in Lin et al. (19), because using either protein alone as a tTreg marker is controversial (19, 39). This method may underestimate the proportion of tTregs, but as tTregs have previously been shown to express both markers, the chosen approach should be superior in discriminating the Treg subtypes. We sought to determine whether the compensation of the peripheral Treg population in Irf4-cKO mice could be influenced by an increased induction of pTregs. There was no change in the distribution of tTregs and pTregs among Tregs either in the thymus or the spleen of Irf4-cKO (Fig. 4A). However, although both pTregs and tTregs were reduced among thymic CD4 SP cells of Irf4-cKO, only pTregs were significantly elevated in the splenic CD4 SP population (Fig. 4B). This rise could be attributed to the higher proportion of activated pTregs but not tTregs of the same subpopulation among Tregs in Irf4-cKO (Fig. 4C). Additionally, discrimination between tTregs and pTregs revealed that the decrease observed in splenic resting Tregs in Irf4-cKO mice (Fig. 3D) reached significance in the resting tTreg but not pTreg population (Fig. 4C).

Despite the peripheral compensation of Tregs in the Irf4-cKO, we found that aged (40–48 wk) but not young (8–10 wk) Irf4-cKO mice developed mild inflammatory lesions. The hematological staining of liver, pancreas, and salivary gland from these mice (Fig. 4D) revealed Irf4-cKO to have elevated susceptibility to mononuclear infiltrations in the salivary gland compared with WT. Although aged WT mice occasionally presented mild salivary gland infiltrations, the infiltrations in the Irf4-cKO were significantly more frequent, with six of eight animals presenting more than one lesion in a single gland (Fig. 4E).

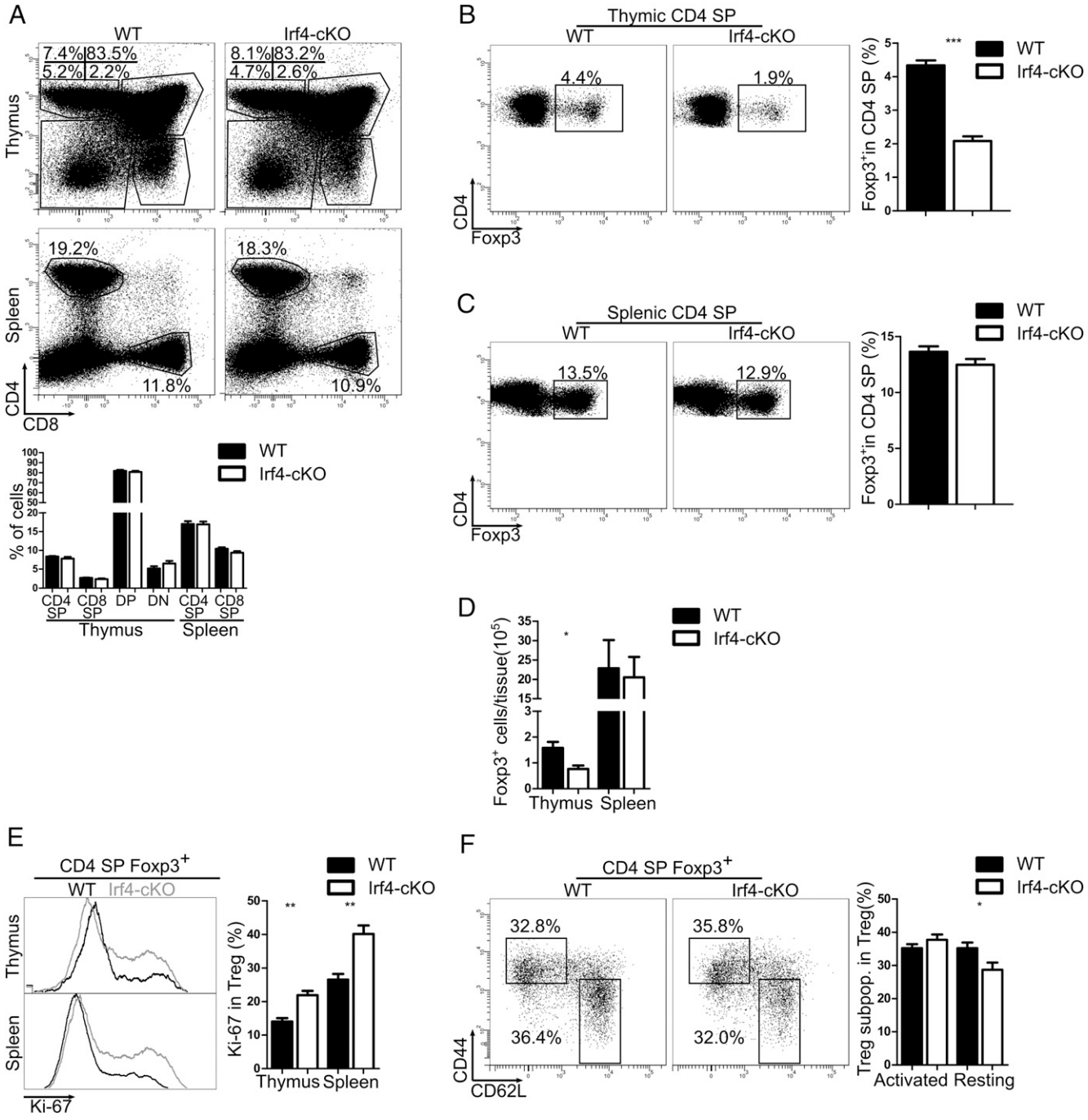

FIGURE 3. Irf4 primes TEC for Treg induction. (**A**) The percentages of thymocyte and splenic T cell populations from WT and Irf4-cKO were evaluated by flow cytometry. Percentages of Foxp3$^+$ Tregs among thymic (**B**) and splenic (**C**) CD4 SP cells were evaluated by flow cytometry. Plots shown (A–C) are representative of three independent experiments (n = 4–6). (**D**) Absolute numbers of Foxp3$^+$ Tregs from the thymi and spleens of WT and Irf4-cKO mice from two independent experiments (n = 4). (**E**) Percentages of Ki-67$^+$ Tregs in WT and Irf4-cKO thymi and spleens. (**F**) Distribution of activated and resting Tregs in the spleens of WT and Irf4-cKO mice. Plots shown (E and F) are representative of two independent experiments (n = 4–6). Data (A–F) are shown as the means + SEM. *$p \leq 0.05$, **$p \leq 0.01$, ***$p \leq 0.001$, unpaired t test, two-tailed.

Irf4-dependent Treg induction capacity develops autonomously of Aire and is associated with altered chemokine and costimulatory molecule expression levels

Several phenotypic features present in Irf4-cKO resembled those of Aire-KO mice, which has mTEC populations skewed toward mTEC^{hi} (40), a reduced thymic Treg population (13, 14), and infiltrations in the salivary gland (among other tissues) (3). The mTEC^{hi} population expressing Aire and Aire-dependent TSA genes has been implicated in Treg differentiation (3), rescue of autoreactive thymocytes from apoptosis, and directing thymocytes toward the Treg lineage (41). Because we found that *Irf4* expression was upregulated in Aire-KO mTEC^{hi} (Fig. 5A), we asked whether the phenotype observed in Irf4-cKO could be due to Irf4 controlling the expression of Aire and its downstream targets. Based on qPCR and flow cytometric analysis, we did not see differences in Aire expression either at the mRNA (Fig. 5B) or protein level (Fig. 5C), with ~40% mTEC^{hi} from both WT and Irf4-cKO expressing detectable levels of Aire protein. Furthermore, although there were

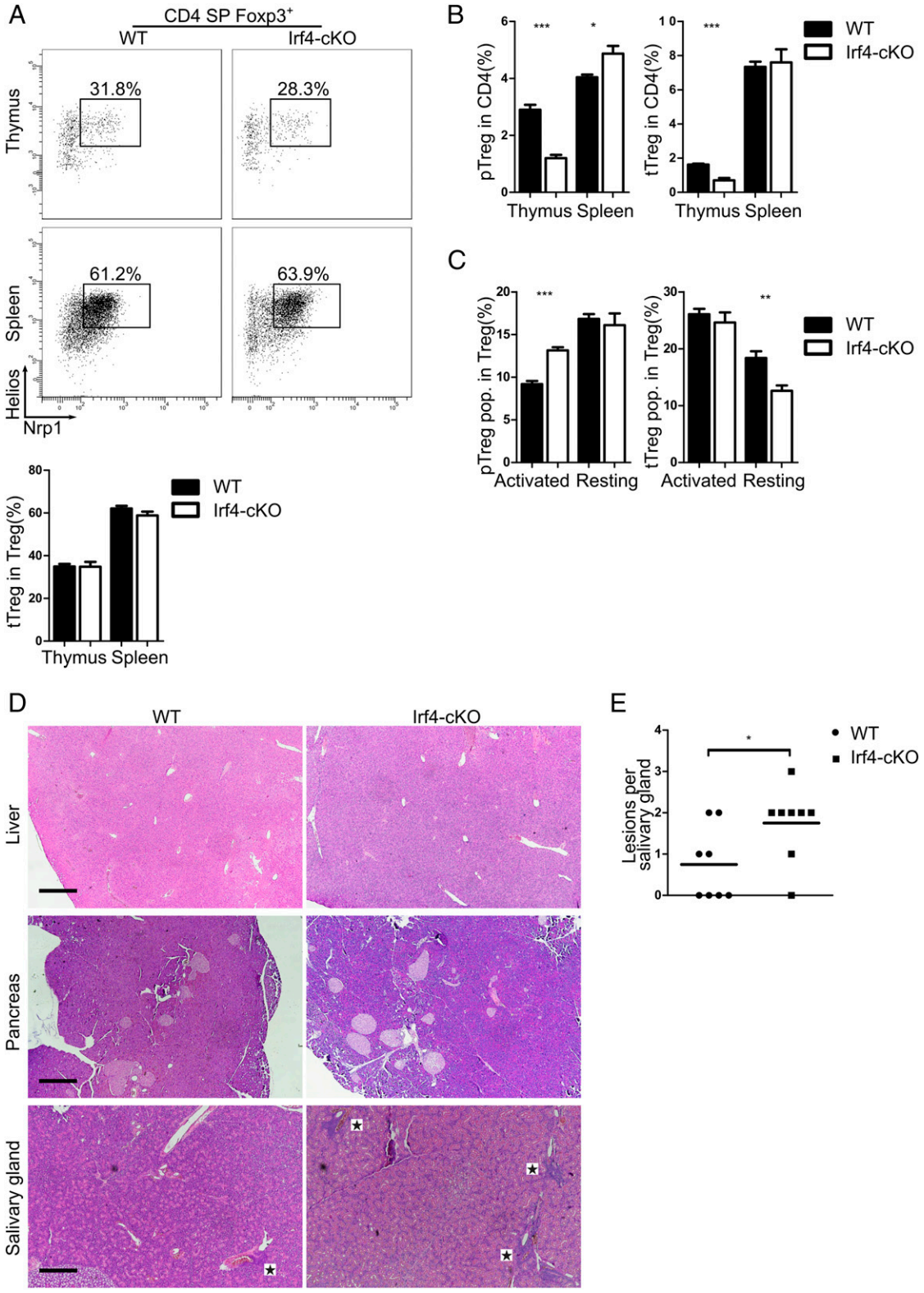

FIGURE 4. Irf4-cKO mice have increased induction of pTregs and mononuclear infiltrations in the salivary gland. (**A**) Distribution of tTregs and pTregs among Tregs in the thymi and spleens of WT and Irf4-cKO was evaluated by flow cytometry. (**B**) Distribution of pTregs and tTregs among thymic and splenic CD4 SP cells was evaluated by flow cytometry. (**C**) Distribution of activated and resting tTregs and pTregs among Tregs in the spleens of WT and Irf4-cKO mice was evaluated by flow cytometry. Plots shown (A) are representative of a single experiment with six mice per genotype. Data (A–C) are shown as the means + SEM from a single experiment with six mice per genotype. $*p \leq 0.05$, $**p \leq 0.01$, $***p \leq 0.001$, unpaired *t* test, two-tailed. (**D**) H&E-stained tissue slides from aged (40–48 wk) WT and Irf4-cKO livers, pancreases, and salivary glands. Infiltrations in the salivary glands are marked with a black star. Images shown are representative of four mice per genotype from two independent experiments. Scale bars, 500 μm. (**E**) Quantitation of salivary gland lesions from aged (40–48 w) WT and Irf4-cKO mice. Data are shown for salivary glands of individual mice with median (horizontal line). $*p \leq 0.05$, Mann–Whitney *U* test, two-tailed.

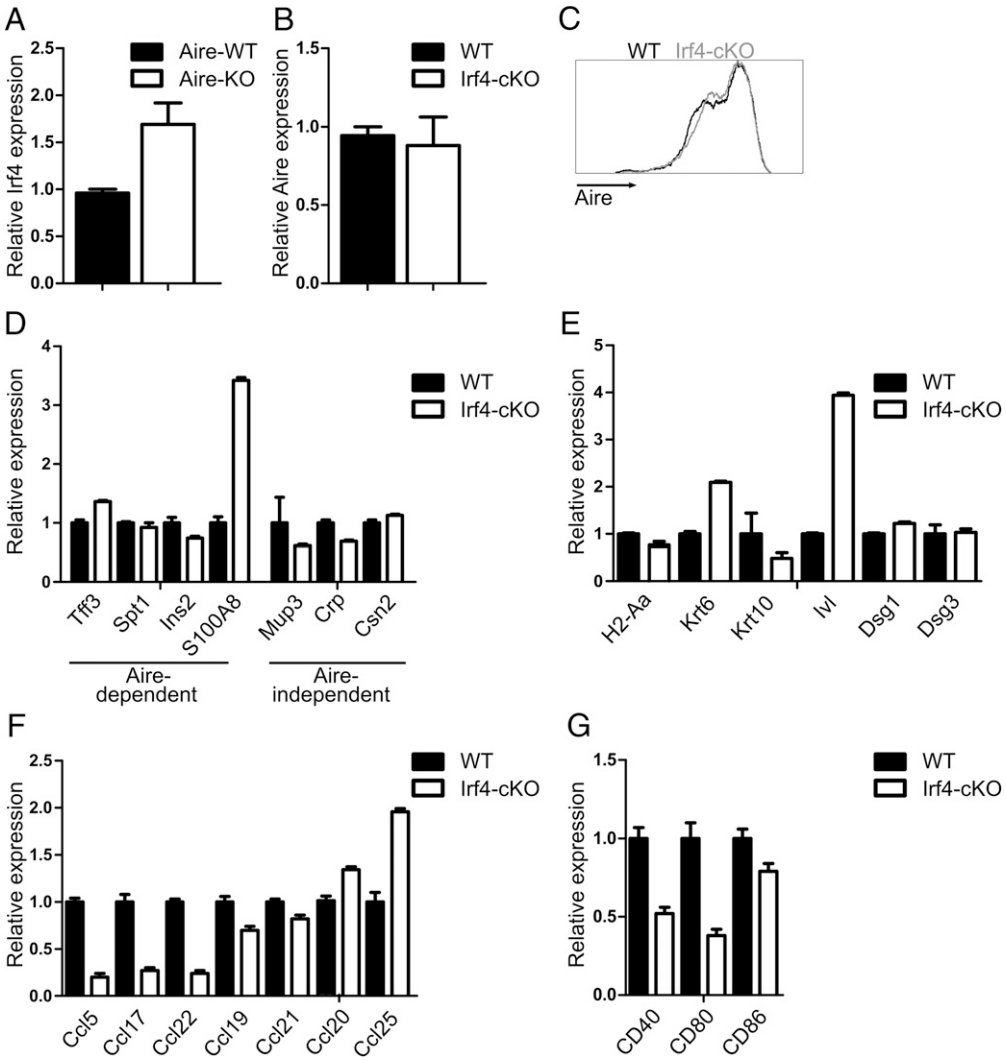

FIGURE 5. Irf4 regulates chemokine and costimulatory molecule expression in mTEC^{hi} independently of Aire. (**A**) Relative expression of *Irf4* mRNA in Aire-KO. (**B**) Relative expression of *Aire* mRNA in Irf4-cKO. Data (A and B) are shown as the means + SEM from two independent experiments from pooled thymi (n = 3–6). (**C**) Aire protein expression was evaluated by flow cytometry in the mTEC^{hi} of WT and Irf4-cKO mice. Plot shown is from a single experiment from pooled thymi (n = 3). Relative expression of Aire-dependent and -independent TSA (**D**) and maturation marker (**E**) mRNA in the sorted mTEC^{hi} of WT and Irf4-cKO was measured by RT-PCR. Relative expression of Aire-dependent chemokine (**F**) mRNA expression in the sorted mTEC^{hi} of WT and Irf4-cKO was measured by RT-PCR. Relative expression of costimulatory molecules (**G**) in the sorted mTEC^{hi} of WT and Irf4-cKO was measured by RT-PCR. Data (D–G) are shown as the means + SEM of three technical replicates from a single experiment from pooled sample (n = 8) and are representative of two experiments.

apparent differences in the expression of Aire-dependent and -independent Ags in mTEC^{hi} of Irf4-cKO (Fig. 5D), there was no clear up- or downregulation of the groups of genes studied in Irf4-cKO. The analysis of mTEC maturation markers dependent on Aire (1, 2) showed that the maturation programs of Irf4-cKO and Aire-KO mice are different (Fig. 5E), as we found decreased expression of the MHC-II molecule *H2-Aa* and increased expression of terminal differentiation markers *Ivl* and *Krt6*, which have been shown to move in opposite directions in Aire-KO (1, 2).

Our analysis of thymocyte subsets showed that the cell populations preceding the CD4 SP Foxp3^{+} phase were similar in the WT and Irf4-cKO mice, suggesting that Irf4 deficiency causes disturbances in the mTEC-specific gene expression profile. Thymocyte migration and Treg induction in thymic medulla depend on the expression of specific chemokines that act as ligands for chemokine receptors expressed on thymocytes (1) and costimulatory molecules such as CD40, CD80, and CD86 (10) by mTEC^{hi} cells. Therefore, we performed qPCR to analyze the gene expression levels of chemokines and costimulatory molecules indicated in thymocyte migration to, and development in, the medulla in the sorted mTEC^{hi} population. We witnessed a steep decrease in the levels of *Ccl5*, *Ccl17*, and *Ccl22* responsible for thymocyte migration into the medulla (Fig. 5F), with smaller but consistent decreases in *Ccl19* and *Ccl21* expression. The levels of *Ccl20* remained unaltered, whereas *Ccl25* was increased in Irf4-cKO. Furthermore, our qPCR analysis of costimulatory molecules revealed a drop in *CD40* and *CD80* expression in Irf4-cKO mice (Fig. 5G) with accompanying small changes in the expression of *CD86*, which shares common receptors on Tregs with CD80.

Collectively, this analysis suggests that the decrease observed in thymic Tregs can be attributed to the altered chemokine and costimulatory molecule expression pattern in the mTEC^{hi} population of Irf4-cKO mice.

Discussion

The mechanisms as to how thymic stromal cells shape Treg induction are unknown. In this study, we presented a pathway by which a cascade of events from RANK signaling to Irf4 expression

and its target genes in mTEC is responsible for the maintenance of the thymic Treg compartment. Our study demonstrates that TEC, a rare population of APC of epithelial lineage, require Irf4 for the maintenance of the mTEC^{lo}/mTEC^{hi} ratio, suggesting that Irf4 is involved in mTEC differentiation. Furthermore, we found that RANK signaling–dependent Irf4 expression is constitutive in thymic epithelium and was the highest in mTEC^{hi}. Taken together, these results provide another example of interdependent maturation and signaling of thymocytes and TEC in the thymus (7–9, 11, 42).

Previous studies have implicated the importance of the classical NF-κB pathway in *Irf4* induction in DC and B cells as well as in T cells (31, 43). RANKL, which modulates *Irf4* expression via the NF-κB pathway, has been described in bone tissue macrophages known as osteoclasts (44) but not in peripheral immune APC. Recently we and others showed that RANK-induced *Aire* expression in the immune system was controlled by the classical NF-κB pathway (45, 46). Our data suggests that *Irf4* expression in TEC is also dependent on the classical NF-κB pathway, as already low concentrations of IKK-β inhibitor that only halved *Aire* expression (45) resulted in a substantial decrease in *Irf4* expression. We cannot exclude the involvement of the alternative NF-κB pathway with full certainty, as inhibiting the alternative pathway also led to a statistically insignificant although considerable reduction in *Irf4* expression.

We found that TEC-specific Irf4 deficiency influenced the maintenance of the thymic Treg population, as we observed a 2-fold decrease in this population in our Irf4-cKO mice. Neither the cTEC population, responsible for thymic positive selection, nor thymocyte populations preceding the CD4 SP Foxp3$^+$ cells were altered in Irf4-cKO. This finding indicates that Irf4 expression in mTEC, rather than cTEC, is needed for Treg induction. As we witnessed a modest yet significant decrease in the splenic resting Treg percentages, we presumed that active compensating mechanisms were present in the periphery restoring Treg homeostasis. Similarly to the thymic Treg population from mice deficient in the conserved noncoding sequence 3 of Foxp3 (47), thymic Tregs in the Irf4-cKO were more prone to Ki-67 expression despite their decreased percentages. It is possible that a proliferation-based compensatory mechanism to recover the Treg niche is already active in the thymi of both of these KO mice, but for some reason it fails. Recirculating Tregs were recently shown to restrain the development of thymic Treg precursors (48). If intact in Irf4-cKO mice, this repressive mechanism, in combination with impaired mTEC-dependent Treg induction, might provide an explanation for the decreased thymic Treg population.

In addition to the increased proliferation rate of Tregs in Irf4-cKO mice, we discovered that peripheral mechanisms have a role in compensating the Treg population in these animals. We demonstrated that the levels of activated pTregs were increased in Irf4-cKO. Additionally, the decrease witnessed in splenic resting Tregs becomes significant only in the resting thymic Treg but not pTreg population. As there were no significant changes in the splenic activated tTreg subpopulation, this decrease in splenic resting tTregs is likely to be the peripheral reflection of decreased thymic Treg production. However, we cannot exclude that homeostatically proliferating Tregs of thymic origin lose expression of Helios and Nrp1 and thereby obtain the pTreg phenotype. Aside from this theoretical possibility, our results indicate that the peripheral homeostatic compensation of the Treg population in Irf4-cKO manifests itself both in the increased proliferation rate of peripheral Tregs as well as higher induction of pTregs.

Although we did not provide a direct link between Treg phenotype in Irf4-cKO and peripheral mononuclear lesions, Tregs generated in thymi lacking Irf4 in TEC could potentially be incapable of suppressing the immune responses, resulting in increased infiltrations in the salivary glands of these mice. The slight yet significant increase in salivary gland infiltrations, observed only in the aged Irf4-cKO mice, might be explained by Irf4 having overlapping functions with Irf8 (38, 49), also expressed in TEC (data not shown), and could therefore ameliorate the phenotype shown in this study. Several features of the phenotype in Irf4-cKO (skewed mTEC populations, decreased thymic Tregs, and increased salivary gland infiltrations) are reminiscent of Aire-KO mice (3, 13, 14, 40), yet our results suggest the two phenotypes to be unrelated. Our immunofluorescence analysis showed no difference in the frequency of Ivl$^+$ cells in Irf4-cKO versus WT, and at the mRNA level, *Ivl* along with *Krt6* were upregulated in Irf4-cKO, indicating that mTEC in Irf4-cKO matured to the post-Aire terminally differentiated TEC. Our results indicate that, unlike in Irf4-deficient B cells and DC (29, 50), MHC-II regulation is compensated for or differentially regulated in Irf4-cKO mTEC^{hi}.

Our expression analysis revealed an altered expression of several chemokines and costimulatory molecules in the mTEC^{hi} of Irf4-cKO, which might provide an explanation for the decreased thymic Treg population. We found that Irf4-cKO had increased levels of *Ccl25*, possibly providing an additional inhibitory effect on Treg development (16), as well as decreased levels of *Ccl5*, *Ccl17*, and *Ccl22* expression. Furthermore, the expression of the costimulatory molecules *CD40* and *CD80*, shown to be crucial for Treg development (10), were substantially decreased in the mTEC^{hi} of Irf4-cKO mice. Although also decreased, the changes in the expression levels of *CD86*, considered largely to be redundant with *CD80*, were considerably smaller, which in turn might explain the unaltered development of SP thymocytes in general.

In conclusion, our study sheds light on the molecular basis of Treg differentiation and on induction of central tolerance. Our results show that these processes require RANK-dependent Irf4 expression in TEC, which in turn regulates the expression of several molecules indicated in Treg induction.

Acknowledgments

We thank Anu Kaldmaa, Maire Pihlap, Liilija Verev, Eve Toomsoo, and Laura Tomson for technical assistance.

Disclosures

The authors have no financial conflicts of interest.

References

1. Laan, M., K. Kisand, V. Kont, K. Möll, L. Tserel, H. S. Scott, and P. Peterson. 2009. Autoimmune regulator deficiency results in decreased expression of CCR4 and CCR7 ligands and in delayed migration of CD4$^+$ thymocytes. *J. Immunol.* 183: 7682–7691.
2. Yano, M., N. Kuroda, H. Han, M. Meguro-Horike, Y. Nishikawa, H. Kiyonari, K. Maemura, Y. Yanagawa, K. Obata, S. Takahashi, et al. 2008. Aire controls the differentiation program of thymic epithelial cells in the medulla for the establishment of self-tolerance. *J. Exp. Med.* 205: 2827–2838.
3. Anderson, M. S., E. S. Venanzi, L. Klein, Z. Chen, S. P. Berzins, S. J. Turley, H. von Boehmer, R. Bronson, A. Dierich, C. Benoist, and D. Mathis. 2002. Projection of an immunological self shadow within the thymus by the aire protein. *Science* 298: 1395–1401.
4. Peterson, P., T. Org, and A. Rebane. 2008. Transcriptional regulation by AIRE: molecular mechanisms of central tolerance. *Nat. Rev. Immunol.* 8: 948–957.
5. Mathis, D., and C. Benoist. 2009. Aire. *Annu. Rev. Immunol.* 27: 287–312.
6. Derbinski, J., J. Gäbler, B. Brors, S. Tierling, S. Jonnakuty, M. Hergenhahn, L. Peltonen, J. Walter, and B. Kyewski. 2005. Promiscuous gene expression in thymic epithelial cells is regulated at multiple levels. *J. Exp. Med.* 202: 33–45.
7. Akiyama, T., Y. Shimo, H. Yanai, J. Qin, D. Ohshima, Y. Maruyama, Y. Asaumi, J. Kitazawa, H. Takayanagi, J. M. Penninger, et al. 2008. The tumor necrosis factor family receptors RANK and CD40 cooperatively establish the thymic medullary microenvironment and self-tolerance. [Published erratum appears in 2013 *Immunity* 39: 796.] *Immunity* 29: 423–437.

8. Hikosaka, Y., T. Nitta, I. Ohigashi, K. Yano, N. Ishimaru, Y. Hayashi, M. Matsumoto, K. Matsuo, J. M. Penninger, H. Takayanagi, et al. 2008. The cytokine RANKL produced by positively selected thymocytes fosters medullary thymic epithelial cells that express autoimmune regulator. *Immunity* 29: 438–450.
9. Rossi, S. W., M. Y. Kim, A. Leibbrandt, S. M. Parnell, W. E. Jenkinson, S. H. Glanville, F. M. McConnell, H. S. Scott, J. M. Penninger, E. J. Jenkinson, et al. 2007. RANK signals from $CD4^+3^-$ inducer cells regulate development of Aire-expressing epithelial cells in the thymic medulla. *J. Exp. Med.* 204: 1267–1272.
10. Williams, J. A., J. Zhang, H. Jeon, T. Nitta, I. Ohigashi, D. Klug, M. J. Kruhlak, B. Choudhury, S. O. Sharrow, L. Granger, et al. 2014. Thymic medullary epithelium and thymocyte self-tolerance require cooperation between CD28–CD80/86 and CD40–CD40L costimulatory pathways. *J. Immunol.* 192: 630–640.
11. Klein, L., B. Kyewski, P. M. Allen, and K. A. Hogquist. 2014. Positive and negative selection of the T cell repertoire: what thymocytes see (and don't see). *Nat. Rev. Immunol.* 14: 377–391.
12. Jordan, M. S., A. Boesteanu, A. J. Reed, A. L. Petrone, A. E. Holenbeck, M. A. Lerman, A. Naji, and A. J. Caton. 2001. Thymic selection of $CD4^+$ $CD25^+$ regulatory T cells induced by an agonist self-peptide. *Nat. Immunol.* 2: 301–306.
13. Malchow, S., D. S. Leventhal, S. Nishi, B. I. Fischer, L. Shen, G. P. Paner, A. S. Amit, C. Kang, J. E. Geddes, J. P. Allison, et al. 2013. Aire-dependent thymic development of tumor-associated regulatory T cells. *Science* 339: 1219–1224.
14. Yang, S., N. Fujikado, D. Kolodin, C. Benoist, and D. Mathis. 2015. Immune tolerance. Regulatory T cells generated early in life play a distinct role in maintaining self-tolerance. *Science* 348: 589–594.
15. Hu, Z., J. N. Lancaster, C. Sasiponganan, and L. I. Ehrlich. 2015. CCR4 promotes medullary entry and thymocyte-dendritic cell interactions required for central tolerance. *J. Exp. Med.* 212: 1947–1965.
16. Evans-Marin, H. L., A. T. Cao, S. Yao, F. Chen, C. He, H. Liu, W. Wu, M. G. Gonzalez, S. M. Dann, and Y. Cong. 2015. Unexpected regulatory role of CCR9 in regulatory T cell development. *PLoS One* 10: e0134100.
17. Sugimoto, N., T. Oida, K. Hirota, K. Nakamura, T. Nomura, T. Uchiyama, and S. Sakaguchi. 2006. Foxp3-dependent and -independent molecules specific for $CD25^+CD4^+$ natural regulatory T cells revealed by DNA microarray analysis. *Int. Immunol.* 18: 1197–1209.
18. Yadav, M., C. Louvet, D. Davini, J. M. Gardner, M. Martinez-Llordella, S. Bailey-Bucktrout, B. A. Anthony, F. M. Sverdrup, R. Head, D. J. Kuster, et al. 2012. Neuropilin-1 distinguishes natural and inducible regulatory T cells among regulatory T cell subsets in vivo. *J. Exp. Med.* 209: 1713–1722.
19. Lin, X., M. Chen, Y. Liu, Z. Guo, X. He, D. Brand, and S. G. Zheng. 2013. Advances in distinguishing natural from induced $Foxp3^+$ regulatory T cells. *Int. J. Clin. Exp. Pathol.* 6: 116–123.
20. Round, J. L., and S. K. Mazmanian. 2010. Inducible $Foxp3^+$ regulatory T-cell development by a commensal bacterium of the intestinal microbiota. *Proc. Natl. Acad. Sci. USA* 107: 12204–12209.
21. Zhao, G. N., D. S. Jiang, and H. Li. 2015. Interferon regulatory factors: at the crossroads of immunity, metabolism, and disease. *Biochim. Biophys. Acta* 1852: 365–378.
22. Cao, Y., H. Li, Y. Sun, X. Chen, H. Liu, X. Gao, and X. Liu. 2010. Interferon regulatory factor 4 regulates thymocyte differentiation by repressing Runx3 expression. *Eur. J. Immunol.* 40: 3198–3209.
23. Huber, M., and M. Lohoff. 2014. IRF4 at the crossroads of effector T-cell fate decision. *Eur. J. Immunol.* 44: 1886–1895.
24. Carreras, E., S. Turner, M. B. Frank, N. Knowlton, J. Osban, M. Centola, C. G. Park, A. Simmons, J. Alberola-Ila, and S. Kovats. 2010. Estrogen receptor signaling promotes dendritic cell differentiation by increasing expression of the transcription factor IRF4. *Blood* 115: 238–246.
25. Gupta, S., M. Jiang, A. Anthony, and A. B. Pernis. 1999. Lineage-specific modulation of interleukin 4 signaling by interferon regulatory factor 4. *J. Exp. Med.* 190: 1837–1848.
26. Matsuyama, T., A. Grossman, H. W. Mittrücker, D. P. Siderovski, F. Kiefer, T. Kawakami, C. D. Richardson, T. Taniguchi, S. K. Yoshinaga, and T. W. Mak. 1995. Molecular cloning of LSIRF, a lymphoid-specific member of the interferon regulatory factor family that binds the interferon-stimulated response element (ISRE). *Nucleic Acids Res.* 23: 2127–2136.
27. Mittrücker, H. W., T. Matsuyama, A. Grossman, T. M. Kündig, J. Potter, A. Shahinian, A. Wakeham, B. Patterson, P. S. Ohashi, and T. W. Mak. 1997. Requirement for the transcription factor LSIRF/IRF4 for mature B and T lymphocyte function. *Science* 275: 540–543.
28. Klein, U., S. Casola, G. Cattoretti, Q. Shen, M. Lia, T. Mo, T. Ludwig, K. Rajewsky, and R. Dalla-Favera. 2006. Transcription factor IRF4 controls plasma cell differentiation and class-switch recombination. *Nat. Immunol.* 7: 773–782.
29. Suzuki, S., K. Honma, T. Matsuyama, K. Suzuki, K. Toriyama, I. Akitoyo, K. Yamamoto, T. Suematsu, M. Nakamura, K. Yui, and A. Kumatori. 2004. Critical roles of interferon regulatory factor 4 in $CD11b^{high}CD8\alpha^-$ dendritic cell development. *Proc. Natl. Acad. Sci. USA* 101: 8981–8986.
30. Satoh, T., O. Takeuchi, A. Vandenbon, K. Yasuda, Y. Tanaka, Y. Kumagai, T. Miyake, K. Matsushita, T. Okazaki, T. Saitoh, et al. 2010. The Jmjd3-*Irf4* axis regulates M2 macrophage polarization and host responses against helminth infection. *Nat. Immunol.* 11: 936–944.
31. Lehtonen, A., V. Veckman, T. Nikula, R. Lahesmaa, L. Kinnunen, S. Matikainen, and I. Julkunen. 2005. Differential expression of IFN regulatory factor 4 gene in human monocyte-derived dendritic cells and macrophages. *J. Immunol.* 175: 6570–6579.
32. Schlitzer, A., N. McGovern, P. Teo, T. Zelante, K. Atarashi, D. Low, A. W. Ho, P. See, A. Shin, P. S. Wasan, et al. 2013. IRF4 transcription factor-dependent $CD11b^+$ dendritic cells in human and mouse control mucosal IL-17 cytokine responses. *Immunity* 38: 970–983.
33. Mecklenburg, L., M. Nakamura, J. P. Sundberg, and R. Paus. 2001. The nude mouse skin phenotype: the role of *Foxn1* in hair follicle development and cycling. *Exp. Mol. Pathol.* 71: 171–178.
34. Han, J., P. Kraft, H. Nan, Q. Guo, C. Chen, A. Qureshi, S. E. Hankinson, F. B. Hu, D. L. Duffy, Z. Z. Zhao, et al. 2008. A genome-wide association study identifies novel alleles associated with hair color and skin pigmentation. *PLoS Genet.* 4: e1000074.
35. Akiyama, T., M. Shinzawa, and N. Akiyama. 2012. TNF receptor family signaling in the development and functions of medullary thymic epithelial cells. *Front. Immunol.* 3: 278.
36. Saito, M., J. Gao, K. Basso, Y. Kitagawa, P. M. Smith, G. Bhagat, A. Pernis, L. Pasqualucci, and R. Dalla-Favera. 2007. A signaling pathway mediating downregulation of *BCL6* in germinal center B cells is blocked by *BCL6* gene alterations in B cell lymphoma. *Cancer Cell* 12: 280–292.
37. Bichele, R., K. Kisand, P. Peterson, and M. Laan. 2016. TNF superfamily members play distinct roles in shaping the thymic stromal microenvironment. *Mol. Immunol.* 72: 92–102.
38. Yamamoto, M., T. Kato, C. Hotta, A. Nishiyama, D. Kurotaki, M. Yoshinari, M. Takami, M. Ichino, M. Nakazawa, T. Matsuyama, et al. 2011. Shared and distinct functions of the transcription factors IRF4 and IRF8 in myeloid cell development. *PLoS One* 6: e25812.
39. Szurek, E., A. Cebula, L. Wojciech, M. Pietrzak, G. Rempala, P. Kisielow, and L. Ignatowicz. 2015. Differences in expression level of Helios and Neuropilin-1 do not distinguish thymus-derived from extrathymically-induced $CD4^+Foxp3^+$ regulatory T cells. *PLoS One* 10: e0141161.
40. Matsumoto, M. 2011. Contrasting models for the roles of Aire in the differentiation program of epithelial cells in the thymic medulla. *Eur. J. Immunol.* 41: 12–17.
41. Malchow, S., D. S. Leventhal, V. Lee, S. Nishi, N. D. Socci, and P. A. Savage. 2016. Aire enforces immune tolerance by directing autoreactive T cells into the regulatory T cell lineage. *Immunity* 44: 1102–1113.
42. Anderson, G., P. J. Lane, and E. J. Jenkinson. 2007. Generating intrathymic microenvironments to establish T-cell tolerance. *Nat. Rev. Immunol.* 7: 954–963.
43. Grumont, R. J., and S. Gerondakis. 2000. Rel induces interferon regulatory factor 4 (*IRF-4*) expression in lymphocytes: modulation of interferon-regulated gene expression by rel/nuclear factor κB. *J. Exp. Med.* 191: 1281–1292.
44. Nakashima, Y., and T. Haneji. 2013. Stimulation of osteoclast formation by RANKL requires interferon regulatory factor-4 and is inhibited by simvastatin in a mouse model of bone loss. *PLoS One* 8: e72033.
45. Haljasorg, U., R. Bichele, M. Saare, M. Guha, J. Maslovskaja, K. Kõnd, A. Remm, M. Pihlap, L. Tomson, K. Kisand, et al. 2015. A highly conserved NF-κB-responsive enhancer is critical for thymic expression of Aire in mice. *Eur. J. Immunol.* 45: 3246–3256.
46. LaFlam, T. N., G. Seumois, C. N. Miller, W. Lwin, K. J. Fasano, M. Waterfield, I. Proekt, P. Vijayanand, and M. S. Anderson. 2015. Identification of a novel cis-regulatory element essential for immune tolerance. *J. Exp. Med.* 212: 1993–2002.
47. Feng, Y., J. van der Veeken, M. Shugay, E. V. Putintseva, H. U. Osmanbeyoglu, S. Dikiy, B. E. Hoyos, B. Moltedo, S. Hemmers, P. Treuting, et al. 2015. A mechanism for expansion of regulatory T-cell repertoire and its role in self-tolerance. *Nature* 528: 132–136.
48. Thiault, N., J. Darrigues, V. Adoue, M. Gros, B. Binet, C. Perals, B. Leobon, N. Fazilleau, O. P. Joffre, E. A. Robey, et al. 2015. Peripheral regulatory T lymphocytes recirculating to the thymus suppress the development of their precursors. *Nat. Immunol.* 16: 628–634.
49. Shukla, V., and R. Lu. 2014. IRF4 and IRF8: governing the virtues of B lymphocytes. *Front. Biol. (Beijing)* 9: 269–282.
50. van der Stoep, N., E. Quinten, M. Marcondes Rezende, and P. J. van den Elsen. 2004. E47, IRF-4, and PU.1 synergize to induce B-cell-specific activation of the class II transactivator promoter III (CIITA-PIII). *Blood* 104: 2849–2857.